RUSSIAN ACADEMY OF SCIENCE
Lenin Order of Siberian Branch
G.I. BUDKER INSTITUTE OF NUCLEAR PHYSICS

Valery S. Cherkassky, Boris A. Knyazev,
Igor A. Kotelnikov and Alexander A. Tyutin

BRAKING OF A MAGNETIC DIPOLE MOVING THROUGH WHOLE AND CUT CONDUCTING PIPES

Budker INP 2005-31

Novosibirsk
2005

Braking of a magnetic dipole moving through whole and cut conducting pipes

Valery S. Cherkassky, Boris A. Knyazev,
Igor A. Kotelnikov and Alexander A. Tyutin

Institute of Nuclear Physics
630090, Novosibirsk, Russia

Abstract

A popular demonstration which often accompanies the introduction of magnetic induction is that in which a magnet is dropped through a long conductive pipe. The induced currents cause a retarding force to dramatically slow the descent of the falling magnet. Here we show that the force is proportional to the velocity v at low velocities but diminishes as v^{-1} or $v^{-1/2}$ when v exceeds some successive thresholds which depend on the conductivity, magnetic permeability and the thickness of the pipe wall. We discuss also the effect of a slit cut in the pipe wall on the magnitude of the retarding force and describe measurements of the magnetic forces and the magnet velocity as function of time in the magnetic braking experiment.

Падение магнитного диполя через сплошную и разрезанную проводящую трубу

Б.А. Князев, И.А. Котельников,
А.А. Тютин, В.С. Черкасский

В известном демонстрационном опыте, часто сопровождающем лекции по электромагнитной индукции, магнит падает через длинную проводящую трубку. Возникающие в трубке токи Фуко создают тормозящую силу, которая существенно замедляют падение магнита. В настоящей работе показано, что тормозящая сила пропорциональна скорости v при малых скоростях, но уменьшается при возрастании скорости сначала пропорционально v^{-1}, а затем пропорционально $v^{-1/2}$. Мы также обсуждаем влияние продольного разреза на величину тормозящей силы и описываем эксперименты по измерению тормозящей силы.

1 Introduction

Descent of a falling magnet in a vertical conducting pipe is a popular demonstration often used in introductory physics courses to illustrate the effect of magnetic induction. Variable flux caused by the falling magnet induces eddy currents in the pipe wall. The currents yield secondary magnetic field, which in turn creates retarding force. The force dramatically reduces magnet velocity in the metallic pipe than it does in ordinary free fall in a nonmetallic pipe.

There are a number of papers where the effect of magnetic braking have been described theoretically and verified experimentally for several conductor configurations: sheet, air track, rotating disc, and pipe [1, 2, 3, 4, 5, 6, 7, 8, 9]. MacLatchy *et al.* [5] gave a simple theory for the retarding force for a magnet in the infinite pipe that appears to be proportional to magnet velocity v. They have calculated the terminal velocity v_∞ of the magnet and recorded the e.m.f. signal experimentally by the use of a multi-turn coil on a copper pipe. Hahn *et al.* [7] have studied oscillations of a magnet attached inside a spring and driven within pipes of different dimension and conductivity through resonance. Their theory is similar to [3, 5], but they took into account finite length of the pipe. Nowadays a variant of the experiment is available commercially (see `http://www.exploratorium.edu/snacks/eddy_currents.html`).

Magnetic braking experiment is used at Novosibirsk State University for many years as a lecture demonstration [10]. When we decided in 2002 to extend the existing set of student experiments adding an experiment with eddy currents, we had reviewed the earlier papers and experimental versions. The review reveals that previous theoretical analysis, besides commonly employed modeling a short magnet as a point magnetic dipole, considered only the case when the skin depth δ is much greater than the wall thickness h, and magnetic permeability of the pipe is equal to unity, $\mu = 1$. These two assumptions can appear not to be valid for many practical situations. It was a reason for development of a general theory for a short magnet moving through a conducting pipe with arbitrary velocity.

The review shows also that in the previous experiments with falling mag-

net all features of this phenomenon cannot be demonstrated. For example, the dynamics of braking was not recorded but only the terminal velocity of the magnet can be measured. The other interesting question, having high education value and was not considered previously, is how the magnet moves through a pipe with a crack or a cut? Will it be the free fall? To our knowledge nobody has analyzed such situation. In this paper we have studied these problems both experimentally and theoretically.

2 The theory

Although a general theory to be described in sec. 2.3 does not need any preliminary assumption on how large is the ratio δ/h, we first describe two limits, $\delta/h \gg 1$ and $\delta/h \ll 1$, and then only we come to the general case. Such approach allows to disclose more clearly the mechanism of the phenomenon and is more instructive for tutorial.

In the next section we reproduce standard theory of the braking experiment valid for low velocities. In sec. 2.2 we consider opposite case of very fast motion of point magnet in conducting pipe and show that the retarding force scales as $v^{-1/2}$ in this case. Then, in sec. 2.3, we develop general theory, which reveals existence of intermediate asymptotes where the force scales as v^{-1}. In the last theoretical section we present a solution for a pipe with a long axial slit.

2.1 Weak skin-effect approximation

When a magnet moves through a pipe in the axial direction, local variation of the magnetic flux induces eddy currents flowing in the azimuthal, or α-, direction (figure 1, *a*). The induced currents create non-uniform magnetic field, which acts back on the magnet with the force

$$\mathbf{F} = (\mathbf{m} \cdot \nabla)\mathbf{B}\,, \tag{1}$$

where $\mathbf{m}$ is a dipole magnetic moment. The force is directed against the velocity of the magnet and, thus, it retards the motion. Further, for definiteness, we refer to the case of falling magnet in gravity field, although the driving force can be of arbitrary nature. Since the retarding force grows as the velocity increases, the magnet reaches eventually a constant velocity at which the retarding force exactly compensates the gravity force.

As stated above, most previous studies of the braking experiment were bounded to a particular case of steady fall. It was usually adopted, explicitly

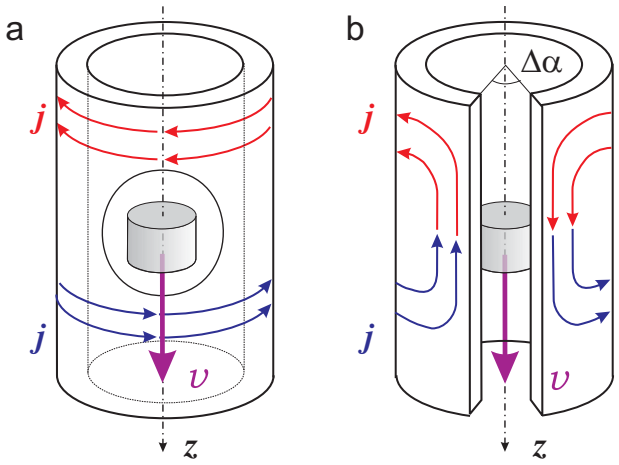

Figure 1: Schematics for the magnet dropping down through a whole (a) and a cut (b) conducting pipe.

or implicitly, that the pipe almost does not perturb the magnetic field of the falling magnet, which, in turn, can be calculated as if the magnet was falling in free space. This assumption is valid 1) for a pipe made of non-magnetic material and 2) for a relatively low velocity v of the motion when the effective skin-depth $\delta = c/\sqrt{2\pi\sigma\omega}$, evaluated for the characteristic frequency $\omega \sim v/a$, is greater than the radius a of the pipe; a more accurate criterium will be formulated later. Our derivation in this section is close to that used in [3] but we modified it to make bridge to the next section, where we consider the case of the strong skin-effect.

Let a spot magnetic dipole $\mathbf{m}$ is directed along the axis z of the circular pipe with the inner radius a and the outer radius b. We assume and that the dipole moves along the axis $r = 0$ and $z_m(t)$ denotes its position at the instant of time t. The axial symmetry of the problem allows to choose such a gauge that the scalar potential ϕ is zero everywhere, and the vector potential $\mathbf{A}$ has only the azimuthal component, $\mathbf{A} = A_\alpha(r, z, t)\,\mathbf{e}_\alpha$. Then non-zero components of the electromagnetic field are

$$B_r = -\frac{\partial A_\alpha}{\partial z}\,, \qquad B_z = \frac{1}{r}\frac{\partial A_\alpha}{\partial r}\,, \qquad E_\alpha = -\frac{1}{c}\frac{\partial A_\alpha}{\partial t}\,. \tag{2}$$

If the skin-effect is weak, the magnetic field of the magnet is almost not perturbed by the conducting wall of the pipe provided that the wall is made

of non-magnetic material, i. e. $\mu = 1$. In the latter case, the vector potential can be calculated within the framework of quasi-static approximation:

$$A_\alpha(r, z, t) = \frac{mr}{[r^2 + (z - z_m)^2]^{3/2}}\,. \tag{3}$$

Noting that $\partial A_\alpha/\partial t = -\dot{z}_m\, \partial A_\alpha/\partial z$, one can readily find the induced electric field E_α within the conducting wall of the pipe. The field drives the eddy current $j_\alpha = \sigma E_\alpha$ that produces "secondary" magnetic field. At the axis z, the magnetic field has only z-component:

$$B_z(0, z) = \frac{1}{c} \int\limits_{-L/2}^{L/2} dz' \int\limits_a^b dr' \, \frac{2\pi r'^2\, j_\alpha(r', z')}{[r'^2 + (z - z')^2]^{3/2}}\,,$$

where $\pm L/2$ are the z coordinates of the ends of the pipe. Differentiating the integrand in the above equation over z and then equating z to $z_m(t)$, one can calculate the gradient of the field at the point of location of the dipole. Multiplying the result by m, we obtain the retarding force:

$$F = -\frac{18\pi\sigma m^2 v}{c^2} \int\limits_{-L/2}^{L/2} dz' \int\limits_a^b dr' \, \frac{r'^3\,(z_m - z')^2}{[r'^2 + (z_m - z')^2]^5}\,, \tag{4}$$

where $v = \dot{z}_m$ stands for the velocity of the magnet. The force does not depend on the coordinate z_m of the dipole if the latter is located far enough from an end of the pipe. If $|z_m \pm L/2| \gg a$, equation (4) reduces to

$$F = -\frac{15\pi^2\sigma m^2 v}{64c^2} \left(\frac{1}{a^3} - \frac{1}{b^3}\right). \tag{5}$$

For a thin pipe, $b - a \ll a$, it reduces even further to the earlier known result of Ref. [3]:

$$F = -\frac{45\pi^2}{64}\, \frac{\sigma m^2 v\, h}{a^4 c^2}. \tag{6}$$

The minus sign here indicates that the force is directed against the velocity of the magnet which justifies the name of the retarding force.

The retarding force can be calculated also from the energy balance treatment. Indeed, the power P, dissipated within conducting wall of the pipe to

the minus sign is equal to the work $A = vF$ executed by the force per unit of time, $-A = P$, and

$$P = \int_{-L/2}^{L/2} dz' \int_a^b d\varrho\, 2\pi\, \varrho\, \sigma E_\alpha^2(\varrho, z')\,.$$

Evaluating the electric field E_α with the use of equations (2) and (3) and dividing the result by $-v$ yields the equation (5) once again. We shall use this latter approach in the next Section to compute retarding force in the limit of fast motion of the magnet.

2.2 Strong skin-effect approximation

Let the velocity of the magnet be so large that the skin depth $\delta = c/\sqrt{2\pi\sigma\mu\omega}$, evaluated at the characteristic frequency $\omega \sim v/a$, is small in comparison with the thickness h of the pipe wall, $\delta \ll h$. To reach such velocity the magnet has to be accelerated by a force different from the gravity one, e. g. in a pneumatic gun or with a spring. The magnetic flux of the magnet in this case is trapped completely inside the pipe, and the eddy currents significantly perturb the magnetic field no matter whether magnetic permeability μ is equal to 1 or not.

Since the motion of the magnet is non-relativistic in any case, $v \ll c$, the magnetic field can still be found with the use of quasi-static approach. It means that the vector potential $A_\alpha = A_\alpha(r, z - vt)$ depends on the time t only through the combination $z - vt$, provide that the dipole is located somewhere far enough from the ends; then $E_\alpha = (v/c)\partial A_\alpha/\partial z$.

At first, we assume that $\delta = 0$, and, consequently, $\mathbf{E} = \mathbf{B} = 0$ inside the pipe wall as well as outside the pipe. Appropriate solution of Maxwell's equation for the interior of the pipe is then subject to the boundary conditions $E_\alpha = B_r = 0$ at the inner radius a of the pipe. In the interior of the pipe, $r < a$, the vector potential obeys the equation

$$\frac{\partial}{\partial r}\frac{1}{r}\frac{\partial}{\partial r} r A_\alpha + \frac{\partial^2}{\partial z^2} A_\alpha = 0 \qquad (7)$$

that follows from the static equation $\nabla \times \mathbf{B} = 0$ for the magnetic field. Eq. (7) has two linear independent particular solutions $\mathrm{I}_1(|kr|)\,\exp(ikz)$ and $\mathrm{K}_1(|kr|)\exp(ikz)$, where I_m and K_m are modified Bessel functions of first and second kind, respectively, of the order m [11]. Since

$$\frac{r}{(r^2 + z^2)^{3/2}} = \frac{2}{\pi}\int_0^\infty dk\, k\, \cos(kz)\, \mathrm{K}_1(kr)$$

the magnetic potential A_α inside the pipe, at $r < a$, can be written in the form

$$A_\alpha \;=\; \frac{2m}{\pi}\int_0^\infty dk\,k\,\cos(kz-kvt)\,[\mathrm{K}_1(kr)+\alpha_k\,\mathrm{I}_1(kr)]\,. \qquad (8)$$

The first terms in the brackets is singular at the point where the spot magnetic dipole is located; it yields the magnetic potential of the magnetic dipole in free space. The second term is regular, and the coefficient α_k can be found from the boundary condition $A_\alpha = 0$ at $r = a$:

$$\alpha_k \;=\; -\,\mathrm{K}_1(ka)/\,\mathrm{I}_1(ka)\,.$$

To find the retarding force at this step it is sufficient to calculate the total power P dissipated within the wall and equate it to the work $-v\,F$ of the retarding force F per unit of time. Dissipated power is equal to the energy flux

$$P \;=\; 2\pi a\int_{-\infty}^{\infty} S_r\,dz \qquad (9)$$

across the entire surface of the inner boundary of the pipe wall, where $S_r = (c/4\pi)E_\alpha H_z$ is the radial component of the Pointing vector at $r = a$. However straightforward calculation shows that $P = 0$ in the current approximation since $E_\alpha = 0$ at $r = a$ and, hence, there is no net energy transfer into the wall. It means that the retarding force disappears when $\sigma \to \infty$ in accordance with a common sense, but in contrast to the result of previous section, which is, thus, valid for relatively slow motion and/or low conductivity.

To accomplish the effect of finite conductivity it is sufficient to use Leontovich boundary condition at the wall surface to relate E_α with H_z. According to Leontovich [12], Fourier amplitude $E_{\alpha\omega} = \int_{-\infty}^{\infty} E_\alpha\,\exp(i\omega t)\,dt$ of the electric field is equal to that of the magnetic field, $B_{z\omega} = \int_{-\infty}^{\infty} B_z\,\exp(i\omega t)\,dt$, times the surface impedance:

$$E_{\alpha\omega} \;=\; [1-\mathrm{sign}(\omega)]\,\sqrt{\frac{\mu|\omega|}{8\pi\sigma}}\,B_{z\omega}\,. \qquad (10)$$

The Fourier component of magnetic field is easily calculated with the use of the longitudinal magnetic field evaluated at $r = a$ for the case $\sigma \to \infty$:

$$B_z \;=\; -\frac{2m}{\pi}\int_0^\infty \frac{dk\,k}{a\,\mathrm{I}_1(ka)}\,\cos(kz-kz_m)\,.$$

This yields

$$B_{z\omega} \;=\; -\frac{2m|k|}{av\,\mathrm{I}_1(|ka|)}\,\exp(-ikz), \tag{11}$$

where $k=\omega/v$. Using the spectrum theorem for the Fourier amplitudes we express the power dissipated within the wall through the Fourier amplitude of the magnetic field $B_{z\omega}$ at the wall:

$$P \;=\; -\frac{acv}{2\pi}\int_0^\infty d\omega\,\sqrt{\frac{\mu\omega}{8\pi\sigma}}\,|B_{z\omega}(a)|^2\,.$$

Inserting here Eq. (11) and dividing the result by $-v$ yields the retarding force:

$$F \;=\; -\frac{m^2c\sqrt{\mu}}{\sqrt{2\pi^3 v\sigma a^9}}\int_0^\infty d\xi\,\frac{\xi^{5/2}}{\mathrm{I}_1^2(\xi)} = -\frac{3.45\,m^2c\sqrt{\mu}}{\sqrt{4\pi\,v\sigma a^9}}\,. \tag{12}$$

Since the force diminishes as v increases, $F\propto v^{-1/2}$, the motion of the magnet is unstable because an occasional increase in the velocity would leads to unlimited acceleration. Similar phenomenon is well known in the plasma physics where high-energy particles are accelerated without limit by an external electric field since friction force is a decreasing function of the particles' velocity. In the next Section we shall see that there is an intermediate asymptotes $F\propto v^{-1}$ in the range $1\ll\delta/h\ll a/\mu\delta$.

2.3 Exact solution

With minor amendments, the method of preceding section can be used to calculate the retarding force in the entire range of parameters of interest.

To derive a general formula, it is sufficient to rewrite eq. (8) in the form

$$A_\alpha(r,z-vt)=\frac{m}{\pi}\int_{-\infty}^{\infty}dk\,\exp[ik(z-vt)]\,|k|[\mathrm{K}_1(|kr|)+\alpha_k\,\mathrm{I}_1(|kr|)] \tag{13}$$

assuming that the coefficient α_k can acquire complex values in the interior part of the pipe, $r<a$. Similar expansions should be written for other regions of the space since in a general case the electromagnetic field diffuses outside the pipe through conducting wall. Outside the pipe, $r>b$, one has to keep only the terms which disappear at $r\to\infty$:

$$A_\alpha(r,z-vt)=\frac{m}{\pi}\int_{-\infty}^{\infty}dk\,\exp[ik(z-vt)]\,\beta_k\,|k|\,\mathrm{K}_1(|kr|)\,. \tag{14}$$

Inside the conducting walls, $a < r < b$, the vector potential obeys the equation

$$\frac{\partial}{\partial r}\frac{1}{r}\frac{\partial}{\partial r} r A_\alpha + \frac{\partial^2}{\partial z^2} A_\alpha = -\frac{4\pi\sigma\mu}{c^2}\frac{\partial A_\alpha}{\partial t}\,, \tag{15}$$

as follows from the equations $\nabla \times \mathbf{H} = 4\pi\mathbf{j}/c$, $\nabla \times \mathbf{E} = -(1/c)(\partial/\partial t)\mathbf{B}$, $\mathbf{j} = \sigma\mathbf{E}$ and $\mathbf{B} = \mu\mathbf{H}$. Solution of the equation can be cast into the form

$$A_\alpha(r,z) = \frac{m}{\pi}\int_{-\infty}^{\infty} dk\, \exp[ik(z-vt)]\,|k|\,[\mu_k\,\mathrm{I}_1(\kappa r) + \nu_k\,\mathrm{K}_1(\kappa r)]\,, \tag{16}$$

where $\kappa = \sqrt{k^2 - 4\pi i k v\sigma\mu/c^2}$.

The coefficients α_k, β_k, μ_k, ν_k are to be found from the boundary conditions at the inner, $r = a$, and at the outer radius of the wall, $r = b$. These conditions imply the continuity of A_α and its derivative $\partial A_\alpha/\partial r$ at both surfaces. To calculate the retarding force one needs only to know the coefficient α_k since

$$F = \frac{m^2}{\pi}\int_0^{\infty} dk\, ik^3\,[\alpha_k - \alpha_{-k}]\,. \tag{17}$$

Simple calculation yields

$$\alpha_k = -\frac{\mathrm{K}_+(a)\,\mathrm{K}_-(b) - \mathrm{K}_-(a)\,\mathrm{K}_+(b)}{\mathrm{I}_-(a)\,\mathrm{K}_-(b) - \mathrm{I}_+(a)\,\mathrm{K}_+(b)}\,, \tag{18}$$

where

$$\begin{aligned}
\mathrm{K}_+(r) &= \kappa\,\mathrm{I}_0(\kappa r)\,\mathrm{K}_1(|k|r) + \mu\,|k|\,\mathrm{I}_1(\kappa r)\,\mathrm{K}_0(|k|r)\,,\\
\mathrm{K}_-(r) &= \kappa\,\mathrm{K}_0(\kappa r)\,\mathrm{K}_1(|k|r) - \mu\,|k|\,\mathrm{K}_1(\kappa r)\,\mathrm{K}_0(|k|r)\,,\\
\mathrm{I}_+(r) &= \kappa\,\mathrm{K}_0(\kappa r)\,\mathrm{I}_1(|k|r) + \mu\,|k|\,\mathrm{K}_1(\kappa r)\,\mathrm{I}_0(|k|r)\,,\\
\mathrm{I}_-(r) &= \kappa\,\mathrm{I}_0(\kappa r)\,\mathrm{I}_1(|k|r) - \mu\,|k|\,\mathrm{I}_1(\kappa r)\,\mathrm{I}_0(|k|r)\,.
\end{aligned}$$

Results of preceding sections, Eqs. (5) and (12), can be recovered from general solution (17) in appropriate limiting cases, though the reduction of (17) is not a trivial task. To derive new results, not discussed earlier, we represent the friction force (17) in the parametric form:

$$F = -\frac{m^2}{a^4}\,\mathcal{F}(\mu,\epsilon,\eta), \tag{19}$$

where the function $\mathcal{F}$ depends on the three dimensionless parameters: μ, $\epsilon = (b-a)/a$ and $\eta = 4\pi\sigma v a/c^2$.

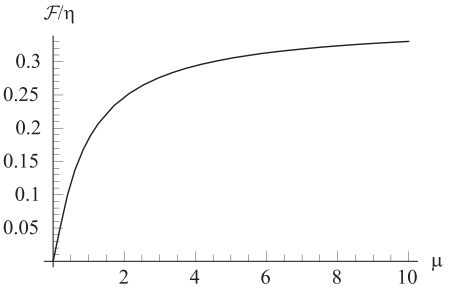

Figure 2: Function $\mathcal{F}$ vs μ for $\eta \ll 1$.

In the case $\eta \ll 1$, which corresponds to the low velocity limit analyzed in Sec. 2.1 with additional assumption $\mu = 1$, general formula (17) can be reduced to comprehensible expression for arbitrary μ if the pipe wall is thick enough, i. e., $\epsilon \gg 1$:

$$\mathcal{F} = \frac{\eta}{\pi} \int_0^\infty \frac{\mu^2 x^4 [\mathrm{K}_2(x)\,\mathrm{K}_0(x) - \mathrm{K}_1^2(x)]}{[1 + (\mu - 1)x\,\mathrm{I}_0(x)\,\mathrm{K}_1(x)]^2}\,. \tag{20}$$

The function (20) is plotted in figure 2. At $\mu = 1$ integration in (20) yields $\mathcal{F} = (15\pi/256)\eta \approx 0.184\eta$ in agreement with (5). At large μ the function (20) tends to the value $\mathcal{F} \approx 0.359\eta$ which is almost 2 times larger. If $\epsilon \ll 1$ one can use the result of Sec. 2.1 since eq. (6) appears to be valid for arbitrary μ. In dimensionless variables eq. (6) takes the form:

$$\mathcal{F} = \frac{45\pi}{256}\,\epsilon\eta \approx 0.552\,\epsilon\eta. \tag{21}$$

The friction force is evidently not very sensitive to the magnetic properties of the pipe wall in the case of slow motion. Apparently, this assertion is valid for an ideal case of the magnet movement precisely along the symmetry axis. Any deviation must lead to the attraction of the magnet to the ferromagnetic wall.

The opposite case of fast motion, analyzed in sec. 2.2, occurs if $\epsilon\eta \gg 1/(\mu\epsilon)$. Then

$$\mathcal{F} = \frac{\sqrt{2\mu}}{\pi\sqrt{\eta}} \int_0^\infty \frac{d\xi\,\xi^{5/2}}{\mathrm{I}_1^2(\xi)} \approx 3.45\sqrt{\frac{\mu}{\eta}} \tag{22}$$

in agreement with (12).

The two cases (21) and (22) do not match each other since there is an intermediate interval of parameters, $1 \ll \epsilon\eta \ll 1/(\mu\epsilon)$, where the friction force scales as v^{-1}:

$$\mathcal{F} = \frac{2}{\pi\epsilon\eta} \int_0^\infty \frac{d\xi\, \xi^2}{\mathrm{I}_1^2(\xi)} \approx \frac{4.78}{\epsilon\eta}\,. \tag{23}$$

The interval exists if $\epsilon \ll 1/\mu$. Within the interval, the width $h = b - a$ of the pipe wall is smaller then the skin-depth, $h \ll \delta$, but exceeds some value, $h \gg \delta^2\mu/a$. The same ordering characterizes the case, when a conducting cylinder effectively screens the electromagnetic field even if $\delta \gg h$ [13, 14].

The diagram in figure 3 illustrates the feasibility of the scalings (22) and (23) for various materials. For a copper pipe with $h/a = 0.25$ the scaling $F \propto v^{-1/2}$ takes place for $va \sim 10^4$ cm^2/s, but $F \propto v^{-1}$ for $va \sim 2{\cdot}10^3$ cm^2/s or less. For $a = 0.665$ cm necessary velocities are 200 m/s and 40 m/s, respectively. For a thick copper pipe with $h = 2.5$ mm and average radius $R = (a+b)/2 = 4$ mm the velocities reduce to 40 m/s and 6 m/s, respectively. Such values can be readily achieved in a simple student experiment.

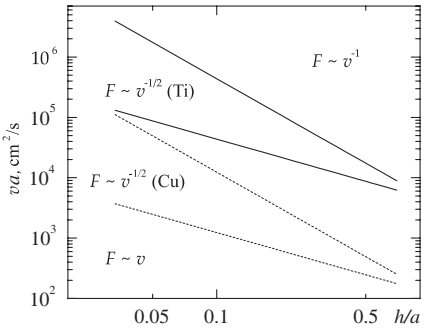

Figure 3: Regions with distinct functional dependence $F(v)$. For a selected material of the wall (titanium or cooper), the region between straight lines corresponds to the scaling $F \propto v^{-1/2}$, whereas $F \propto v$ below the lower line, and $F \propto v^{-1}$ above the upper line.

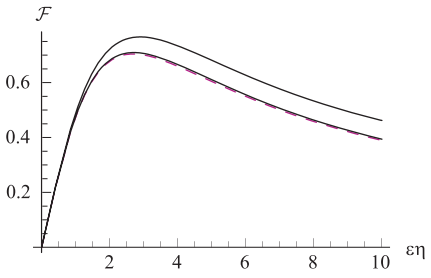

Figure 4: Retarding force for a conducting pipe with thin walls. Dashed line shows approximate solution (24) valid in the limit $\epsilon \to 0$ in the entire range $\epsilon\eta \ll 1/(\mu\epsilon)$. Solid lines show exact solutions at $\mu = 1$ for two values of ϵ: $\epsilon = 0.1$ (upper curve) and $\epsilon = 0.01$ (very close to dashed curve).

The entire range $\epsilon\eta \ll 1/(\mu\epsilon)$ is covered by the formula

$$\mathcal{F} = \frac{2\epsilon\eta}{\pi} \int_0^\infty \frac{d\xi\, \xi^4\, \mathrm{K}_1^2(\xi)}{1 + \epsilon^2\eta^2\xi^2\, \mathrm{I}_1^2(\xi)\, \mathrm{K}_1^2(\xi)}\,. \tag{24}$$

It can be derived from "first principles" if one neglects the variation of A_α (and hence variation of current density) across the pipe wall. To obtain (24), it is sufficient to treat the pipe wall as infinitesimally thin circular layer and match the solutions inside (34) and outside the pipe (35) through the boundary conditions $E_\alpha(a+0) - E_\alpha(a-0) = 0$ and $B_z(a+0) - B_z(a-0) = -4\pi I/c$, where $I = \sigma h E_\alpha(a)$ is the total current per unit length of the pipe wall. The function (24) is plotted in figure 4.

Note that for a thin wall, $\epsilon \ll 1$, the friction force is not sensitive to the magnetic properties of the pipe wall (i.e., to the magnitude of μ) and depends on the other two parameters ϵ, η only through their product if $\epsilon\eta \ll 1$. It reaches maximal magnitude $\mathcal{F} = 0.704$ at $\epsilon\eta = 2.69$.

To build up a bridge to experiment we restrict ourselves below to the case, comprehensively described by eq. (24), assuming that $\epsilon \ll 1$ and $\epsilon\eta \ll 1/(\mu\epsilon)$. In dimensional units these inequalities are transformed into $h \ll a$ and $h \ll \delta$, respectively, where $\delta \sim c/\sqrt{2\pi\sigma\mu v/a}$.

2.4 Pipe with longitudinal slit

The longitudinal slit tears azimuthal current circulating within a pipe wall. However there are two effects that sustain the current. First of all, the displacement current $-(1/c)\partial\mathbf{E}/\partial t$ is capable, in principle, to shorten conductivity current across the slit but this effect is negligible at low velocities. Second effect is more important. Since the eddy currents, driven by e.m.f., are directed in opposite directions in front of moving magnet and behind the magnet (see figure 1), they can re-connect to each other along the slit shores. In the quasi-static approximation no net electric charge is induced in the bulk of the conducting wall, but the electric charge has to be distributed over the surface of the wall to provide closing of the current.

Within the wall

$$\mathbf{E} = \frac{v}{c}\,\frac{\partial A_\alpha}{\partial z}\,\mathbf{e}_\alpha - \nabla\phi, \tag{25}$$

where $A_\alpha = mr/[r^2 + (z - vt)^2]^{3/2}$ is the vector potential of the spot magnetic dipole m in free space, and ϕ is the scalar (electric) potential induced by the surface charges. The potential ϕ obeys the Laplace's equation $\Delta\phi = 0$ in

the bulk of the wall. For a thin wall, $h \ll a$, the Laplace's equation can be considerably simplified since there is no radial electric field within the wall, $\partial\phi/\partial r = 0$. Thus, we have the equation

$$\frac{1}{a^2}\frac{\partial^2\phi}{\partial\alpha^2} + \frac{\partial^2\phi}{\partial z^2} = 0, \tag{26}$$

where we have substituted the variable r with the pipe radius a. The absence of the radial electric field follows from the boundary condition for the density current

$$\mathbf{j} = \sigma\mathbf{E} \tag{27}$$

that must disappear at the boundary of conducting material as long as one can neglect the displacement current. We seek the solution of eq. (26) in the form

$$\phi(\alpha, z) = \int_0^\infty dk\, \sin(kz - kvt)\, \left[\mu_k \exp(ka\alpha) + \nu_k \exp(-ka\alpha)\right], \tag{28}$$

where the coefficients μ_k, ν_k are to be found from the boundary condition for the density current which states that $j_\alpha = 0$ at both edges of the slit.

We denote the angle width of the slit by $\Delta\alpha$ (see figure 1) and assume that the edges of the slit are located at $\alpha = \pm(\pi - \Delta\alpha/2)$. This yields

$$\mu_k = -\nu_k = -\frac{mv}{\pi c}\,\frac{k\,\mathrm{K}_1(ka)}{\cosh[(\pi - \Delta\alpha/2)ka]}. \tag{29}$$

Power dissipated within the conducting wall is equal to

$$P = h \int_{-\pi+\Delta\alpha/2}^{\pi-\Delta\alpha/2} d\alpha\, a \int_{-\infty}^{\infty} dz\, [j_\alpha^2 + j_z^2]/\sigma\,, \tag{30}$$

where the components j_α, j_z of the current density can be readily found by combining Eqs. (27), (25), (28), and (29):

$$\begin{aligned} j_\alpha &= \frac{2m\sigma v}{\pi c} \int_0^\infty dk\, k^2\ \mathrm{K}_1(ka)\ \sin[k(z - vt)]\, \frac{\cosh[ka\alpha] - \cosh[(\pi - \Delta\alpha/2)ka]}{\cosh[(\pi - \Delta\alpha/2)ka]}\,, \\ j_z &= \frac{2m\sigma v}{\pi c} \int_0^\infty dk\, k^2\ \mathrm{K}_1(ka)\ \cos[k(z - vt)]\, \frac{\sinh[ka\alpha]}{\cosh[(\pi - \Delta\alpha/2)ka]}\,. \end{aligned} \tag{31}$$

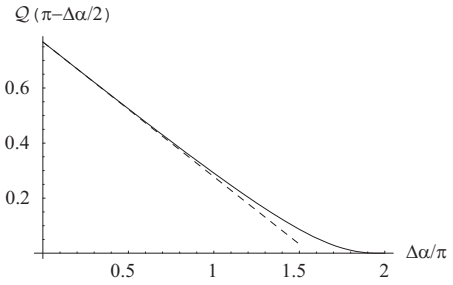

Figure 5: The function $\mathcal{Q}(\Delta\alpha)$ (solid line) and its linear approximation (dashed line).

Integration over z and α in Eq. (30) can be done in a closed form. Dividing the result by $-v$, we find the retarding force:

$$\mathcal{F} = -\frac{45\pi}{256}\,\mathcal{Q}(\pi - \Delta\alpha/2)\,\epsilon\eta\,, \tag{32}$$

where

$$\mathcal{Q}(\beta) = \frac{512}{45\pi^3}\int_0^\infty d\xi\,\xi^3\,\mathrm{K}_1^2(\xi)\,[\beta\xi - \tanh(\beta\xi)]\ .$$

The function $\mathcal{Q}(\pi - \Delta\alpha/2)$ gives the ratio of the retarding forces in the pipe with and without a slit; it is plotted in figure 5. With accuracy to within few percent it can be approximated by a linear function

$$\mathcal{Q}(\pi - \Delta\alpha/2) \approx 0.77 - 0.16\Delta\alpha\,, \tag{33}$$

if $\Delta\alpha \leqslant 3\pi/2$.

3 The experiment

We have studied a magnet falling down through vertical conducting pipes in the gravity field. This experiment corresponds to the slow velocity case, $\eta \ll 1$.

Experimental setup consists of a set of vertical pipes with the length $L = 90\,\mathrm{cm}$ made of copper, aluminum alloy, brass, titanium and a glass pipe for reference. The pipes were taken from the stock and have no certificates. Pipe dimensions are given in table 1. A cylindrical neodymium-iron-boron

Table 1: Pipe characteristics (outer and inner diameters, $2a$ and $2b$, aperture angle, $\Delta\alpha$, and the conductivity, σ) and main experimental results. Values of the conductivity σ for copper and titanium are taken from standard tables. Conductivities for aluminium alloy and brass are calculated using equation (36). The friction coefficients β, initial velocity v_1 of the magnet at first measuring coil and the magnetic moment m_t are obtained with the use of time-flight fitting procedure, based on equation (35). The magnitude of v_1 is shown in bold figures if it is equal to the terminal velocity v_∞. Magnetic moment m_U is obtained in the result of fitting experimental oscillograms with calculated voltage (37).

	Cu	Al	Al	Al	Brass	Ti	Glass
$\Delta\alpha$, rad	none	none	0.32	$\pi/4$	none	none	none
$2a$, mm	11.6	12.4	12.4	12.4	11.7	11.9	11.8
$2b$, mm	15.0	16.0	16.0	16.0	13.9	14.3	15.0
σ, $10^{17}\,\mathrm{s}^{-1}$	5.27	*1.74*			*1. 35*	0.192	-
β, s^{-1}	143.	38.0	31.3	23.0	27.2	3.8	0.137
v_1 ($\boldsymbol{v_\infty}$), $\mathrm{cm\,s}^{-1}$	**6.85**	**25.8**	**31.3**	**42.6**	**36.1**	116.	140.1
m_t, $\mathrm{g}^{1/2}\,\mathrm{cm}^{5/2}\,\mathrm{s}^{-1}$	474 ± 2	-	-	-	-	465 ± 5	-
m_U, $\mathrm{g}^{1/2}\,\mathrm{cm}^{5/2}\,\mathrm{s}^{-1}$	433	429	-	-	425	436	429

magnet with a diameter of 1 cm and a length of 1 cm is magnetized along the axis. The magnet starts at zero velocity from the upper end of a pipe. Seven 20-turn coils, each 8 mm in length, are connected in series and winded on the outer surface of the pipes with a period of 10 cm. The coil series is connected to a digital Tektronix TDS-220 oscilloscope coupled to PC.

3.1 Falling of the magnet through a whole pipe

Voltage $U(t)$ vs. time from the coil series for glass, titanium and aluminum alloy pipes are shown in figure 6. It is clear that the signals are proportional to eddy currents at the outer surface of the pipe wall. The spikes on the oscillograms are evidently produced by e.m.f. induced in the coil, nearest to an instant position of the falling magnet. Since $U(t) = 0$ when the magnet passes the center of a coil, the time of flight from a coil to a neighboring coil can be readily determined from the oscillograms. The result of the time-flight processing is shown in figure 7, where the time of flight through the upper measuring coil is taken to be zero. The $t-z$ diagram is plotted by averaging over 12 individual experiments for each pipe. Experimental errors are

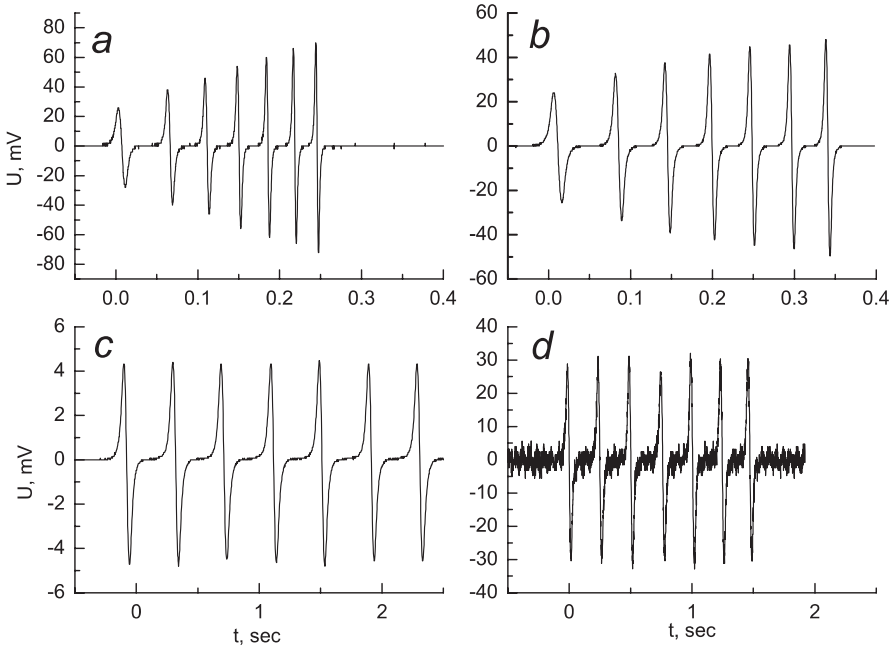

Figure 6: Voltage induced in the measuring coil series: a—glass, b—titanium, c—aluminum alloy, d—aluminum alloy with a longitudinal cut $\Delta\alpha = \pi/2$. A series of 7 coils is wound on every pipe with the period 10 cm. The oscillograms for the copper, brass, and aluminum alloy ($\Delta\alpha = 0.32$) pipes are similar to the oscillograms c and d.

negligible in comparison with the point size. For the copper pipe, possessing the best conductivity, the magnet passes 70 cm for about 9 s, a while very impressive for public demonstrations. Electrical conductivity of the titanium pipe is 20 time less, and time of flight diminishes to 0.35 s. The skin depth δ evaluated at the characteristic frequency $\omega \sim v/a$ for all the pipes is equal or even exceeds few centimeters, which justifies the use of the weak skin-effect approximation in the calculations below. In this approximation, the retarding force can be written as $F = -\beta M \dot{z}_m$, where β is the magnetic friction coefficient, $M = 5.5\,\mathrm{g}$ is the mass, and $z_m(t)$ is an instant coordinate of the magnet. Solving the equation of motion for the magnet in the gravity field

$$\ddot{z}_m(t) + \beta \dot{z}_m(t) \quad = \quad g\,, \tag{34}$$

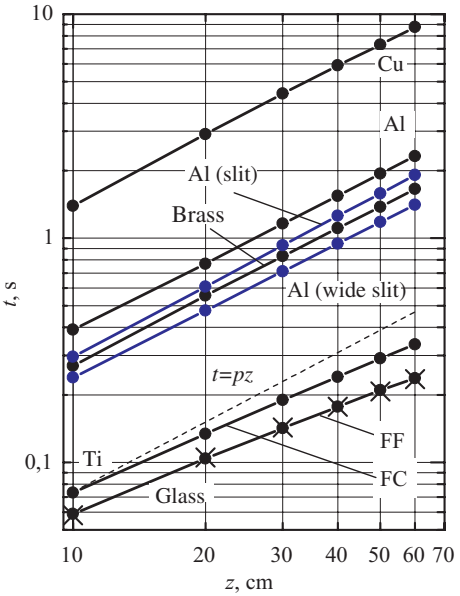

Figure 7: Transit time vs. coordinates of measuring coils. Circles denote instants of time when the magnet passes through a measuring coil. Solid curves designate theoretical trajectory (34) fitted over the friction coefficient β and initial velocity v_1. The curve FF for the glass pipe with high accuracy corresponds to the free fall. The other curves correspond to the motion with constant velocity, besides the curve FC for titanium pipe that exhibits the intermediate case of slowing descending.

with the initial conditions $z_m(0) = 0$, $\dot{z}_m(0) = v_1$ yields

$$z_m(t) = \frac{gt}{\beta} - \frac{g - \beta v_1}{\beta^2} \left[1 - \exp(-\beta t)\right], \tag{35}$$

where v_1 is the velocity of the magnet at the center of the first coil.

We used the equation (34) to fit the experimental data shown in figure 7. Excepting titanium and glass pipes, the experimental data fit the straight line $t = z/v_\infty$, because the magnet brakes down to the terminal velocity $v_\infty = g/\beta$ very soon after entry into the highly conducting pipes before it reach the first measuring coil; for such pipes $v_1 = v_\infty$. The magnet falls down practically free through the glass tube as the fitting curve FF demonstrates in figure 7. The curve FC for titanium exhibits intermediate case when all the term in the equation (34) are equally important.

Having found the friction coefficients β, one can readily calculate the magnetic dipole moment, if the electrical conductivity of the pipe is known, since

$$m_t = \sqrt{\frac{64\beta M R^4 c^2}{45\pi^2 \sigma h}} \tag{36}$$

as follows from the equation (6).

Compiling data for conductivity from many standard tables, we assume the conductivities to be $\sigma = (5.27 \pm 0.03) \cdot 10^{17}$ s^{-1} for copper and $\sigma = (1.92 \pm 0.04) \cdot 10^{16}$ s^{-1} for titanium. Calculated magnitude of the magnetic momentum m_t are given in table 1; the two values of m_t for the copper and titanium pipes reasonably fit each other. Note however that statistical dispersion of the calculated magnetic moment m_t is less than the uncertainty in the used conductivity values.

Inserting the average value of the calculated magnetic momentum $\langle m_t \rangle = (169.5 \pm 5.5)\,\mathrm{g}^{1/2}\,\mathrm{cm}^{5/2}\,\mathrm{s}^{-1}$ in Eq. (36), we have calculated the conductivity for other non-cut pipes. The values $\sigma = 1.35 \cdot 10^{17}$ s^{-1} for brass and $\sigma = 1.74 \cdot 10^{17}$ s^{-1} for aluminum alloy, found in this way, are within the ranges of the conductivity for these materials, given in many handbooks.

Last line in the table contains the values of the magnetic moment m_U calculated with the use of an alternative method. In this method, an experimental oscillogram is approximated by the calculated voltage

$$U(t) = \frac{6\pi m \rho}{c}\, \dot{z}_m(t) \sum_{i=1}^{7} \sum_{j=1}^{20} \frac{\rho (z_m(t) - z_{ij})}{[(z_m(t) - z_{ij})^2 + \rho^2]^{5/2}}\,, \tag{37}$$

where $\rho = b + d/2$ is a coil radius, d is the wire diameter, z_{ij} is the coordinate of a coil turn, and $z_m(t)$ is the coordinate of the magnet as a function of time obtained in the result the fitting procedure, described above. The summation in (37) goes over every of seven coils with 20 turns each. For the given function $z_m(t)$, the voltage function (37) contains single fitting parameter m. This fact drastically simplifies fitting procedure, which incidently does not require knowledge of the conductivity of the material. The described procedure yields practically identical values of m_U for all the pipes presented in table 1, from copper one to glass. However average value $\langle m_U \rangle$ of m_U is 10% less than $\langle m_t \rangle$. Second method that yields m_U is supposed to be more reliable since it is based of less number of assumptions and gives consistent results independently on whether braking is effective (for the good conductors) or not (for the glass pipe).

3.2 Falling of the magnet through a pipe with longitudinal slit

When a pipe has a longitudinal crack or cut, eddy current distribution in the wall drastically change. As it was shown in sect. 2.4, eddy currents below and above the magnet, which are separate in the whole pipe, form in the cut pipe the configuration drawn in figure 1,*b*. As a consequence, the retarding force decreases. According to (32) and (33), the friction coefficient β for the aluminum alloy pipes with narrow ($\Delta\alpha = 0.32$) and wide ($\Delta\alpha = \pi/4$) slits should have the magnitude $\beta_{th} = 27.6\,\mathrm{s}^{-1}$ and $20.4\,\mathrm{s}^{-1}$, respectively. However, experimental values are (10–15)% greater (see table 1).

A simple explanation suggests itself "by ear". One hears a specific raspy sound when the magnet descends inside the pipe with slit, while no sound is heard when the magnet falls throughout the uncut pipe. This means that the magnet scratches the inner surface of the wall if there is a slit cut but otherwise does not touch the wall. Since the slit breaks azimuthal symmetry of the pipe, the eddy currents flowing along the opposite edges of the slit create magnetic field $\mathbf{B}_\perp$ directed to the slit at instant position of the magnet. The field yields the torque $\mathbf{K} = \mathbf{m} \times \mathbf{B}_\perp$, which rotates the magnet in the plane passing from the center of the magnet to the middle of the slit. Since the diameter of the magnet was merely two millimeter smaller than the inner diameter of the pipe, the torque presses opposite edges of the magnet to the inner surface of the wall, and total retarding exceeds the friction force predicted by equation (32).

To demonstrate this effect we cut four slots with the length of 12 cm in a long aluminum pipe with the total length 110 cm alternated with 12-cm uncut sections. The slots had different angular widths, sequentially $\Delta\alpha/\pi = 0.2, 0.1, 0.05, 0.025$. Twenty seven measuring coils were wound in series on the pipe with 4-cm period. Characteristic oscillogram and the magnet velocity as function of time are shown in figure 8. Movement of the magnet in this pipe is rather slow, and the experiment gives clear evidence that the raspy sound appears, when the magnet passes the slots, and disappears, when the magnet is in the uncut sections. The magnet terminal velocity keeps a constant value within all uncut sections, but in the cut sections velocity is not monotonically decreases for the subsequently narrowing slots, as one can expect from Eq. (32) ignoring additional wall friction.

Total retarding force in the cut section is the sum of magnetic braking and mechanical wall friction. We suggest that non-monotonicity of the measured retarding force is explained by non-monotonic dependance of the torque K on the slit width. Using the solution (31) for current in the pipe wall one can

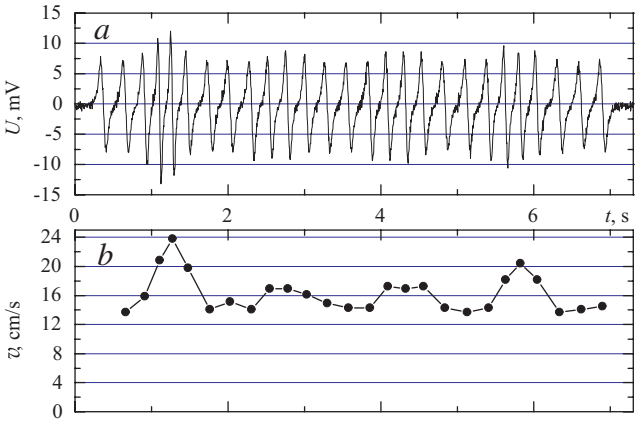

Figure 8: Falling of the magnet in the pipe with sequence of longitudinal slots: (a) oscillogram of the signal from the series of 27 measuring coils; (b) magnet velocity vs. time retrieved from the oscillogram. When the pipe is rotated by 180° around a horizontal direction, the oscillogram remains absolutely the same with t-axis directed from right to left.

find that

$$K = \frac{m^2}{a^3}\,\frac{45\pi}{256}\,\mathcal{K}\big(\pi - \tfrac{1}{2}\Delta\alpha\big)\,\epsilon\eta\,, \tag{38}$$

where

$$\mathcal{K}(\chi) = \frac{512}{45\pi^3}\int_0^\infty dy\,\frac{y^3}{1+y^2}\,\mathrm{K}_1(y)\,[y\,\mathrm{K}_0(y) + \mathrm{K}_1(y)]\,[y\sin\chi - \cos\chi\,\tanh(\chi y)]\,.$$

A ratio of the pressure force, which acts on the wall at each side of the magnet, to the retarding force (21), which acts on the magnet in the whole pipe, is proportional to the function $\mathcal{K}$. Mechanical friction force $F = kN$ is proportional to N and corresponding friction coefficient k which is usually less than unity, $k < 1$. As it is seen from figure 9, the torque reaches maximum at $\Delta\alpha = 0.53\pi = 96°$. Depending of the value of k, the maximum of the total retarding force can be reached at a smaller angular width of the slit. Such peculiarity may qualitatively explain velocity variations observed in our experiment with the multi-slot pipe. Other effect that also may increase the friction force is increasing the magnet rotation angle with cut widening.

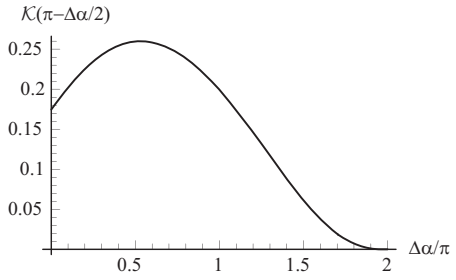

Figure 9: The function $\mathcal{K}(\Delta\alpha)$.

4 Conclusion

Thoroughly investigation of the problem of magnet braking in a conducting pipe appears to be much more instructive than it is usually thought of. We found that apart the regime of slow motion, characterized by linear proportionality of the retarding to the magnet speed, there are two more regimes, where the force decreases as the velocity grows. Similar phenomenon in plasma physics is known to lead to unlimited acceleration of fast electrons in current-carrying plasma.

Performed experiments showed that magnet braking can be used for detection of cracks in the pipes. They also revealed a peculiarity in the dependance of velocity on the slit width. The peculiarity appears due to rotation of the magnet in the magnetic field, perturbed by the axial component of eddy current on opposite shores of the slit.

Thus, a simple magnet braking experiment can be used to introduce students into entirely new field of study. It can be useful at different levels of education, from beginners to postgraduates. One can suggest even more sophisticated experiments on magnetic braking than it is usually done. In particular, new theoretically predicted regimes, where the retarding force is a decreasing function of the magnet speed, are still subject to experimental proof.

Acknowledge

Authors are thankful to P.D. Vobly, who provided us with the magnet, and to G.V. Meledin and A.N. Matveenko for helpful discussions.

References

[1] Marcuso M, Grass R, Jones D and Rowlett C. 1991, *Am. J. Phys.* **59**, 1118.

[2] Marcuso M, Grass R, Jones D and Rowlett C. 1991, *Am. J. Phys.* **59**, 1123.

[3] Saslow W.M. 1992, *Am. J. Phys.* **60**, 693.

[4] Ribarić M and Ŝuŝterŝiĉ L. 1992, *Am. J. Phys.* **23**, 127,

[5] MacLatchy C S, Backman P and Bogan L. 1993, *Am. J. Phys.* **61**, 1096.

[6] Cadwell L.H. 1996, *Am. J. Phys.* **64**, 917.

[7] Hahn K D, Johnson E M, Brokken A and Baldwin S. 1998, *Am. J. Phys.* **66**, 1066.

[8] Kraftmakher Y. 2001, *Eur. J. Phys.* **22**, 477.

[9] Redžić. 2002, *Eur. J. Phys.* **23**, 127.

[10] Meledin G.V. Private communication, 2002.

[11] Janke-Emde-Lösch. 1960, *Tafeln höherer Funktionen* (B.G. Teubner Verlagsgesellschaft, Stutgart), p.245.

[12] Landau L.D. and Lifshits E.M. 1982, *Theoretical Physics: Electrodynamics of the Continuous Media* (Moscow: Nauka), p.414 (in Russ.).

[13] Fathy S, Kittel C, and Louie S.G. 1988, *Am. J. Phys.* **56**, 989.

[14] Cherkassky V.S., Knyazev B.A., Kotelnikov I.A., 2003, *Electromagnetic screening by a thin conducting can* (Preprint Budker Institute of Nuclear Physics BINP 2003-71, Novosibirsk, 2003, 15 p.).

Valery S. Cherkassky, Boris A. Knyazev,
Igor A. Kotelnikov and Alexander A. Tyutin

Braking of a magnetic dipole moving through whole and cut conducting pipes

Б.А. Князев, И.А. Котельников,
А.А. Тютин, В.С. Черкасский

Падение магнитного диполя через сплошную и разрезанную проводящую трубу

Budker INP 2005-31

Ответственный за выпуск А.М. Кудрявцев
Работа поступила 2.06.2005 г.

Сдано в набор 7.06.2005 г.
Подписано в печать 8.06.2005 г.
Формат бумаги 60×90 1/16 Объем 1.5 печ.л., 1.2 уч.-изд.л.
Тираж 110 экз. Бесплатно. Заказ № 31

Обработано на IBM PC и отпечатано на
ротапринте ИЯФ им. Г.И. Будкера СО РАН
Новосибирск, 630090, пр. академика Лаврентьева, 11.